

# Unimolecular decay of the thiomethoxy cation, $\text{CH}_3\text{S}^+$ : A computational study on the detailed mechanistic aspects

Massimiliano Aschi<sup>a)</sup> and Felice Grandinetti

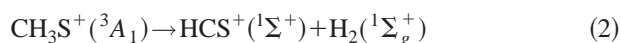
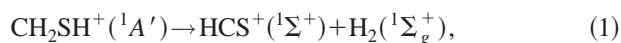
*Dipartimento di Scienze Ambientali, Università della Tuscia, Via S. C. De Lellis, 01100 Viterbo, Italy*

(Received 5 March 1999; accepted 9 July 1999)

The unimolecular decay of the triplet thiomethoxy cation  $\text{CH}_3\text{S}^+$ , ion **1**, has been investigated by density functional theory, *ab initio*, and Phase-space/Rice Ramsperger Kassel Marcus (PST/RRKM) calculations. We have first located on the singlet and triplet B3LYP/6-311+G(*d,p*)  $[\text{C,H}_3,\text{S}]^+$  potential energy surfaces the energy minima and transition structures involved in the lowest energy decompositions of **1**, including the loss of H,  $\text{H}_2$ , and S. We have subsequently located the minimum energy points lying on the B3LYP/6-311+G(*d,p*) hyperline of intersection between the singlet and triplet surfaces, using a recently described steepest descent-based method [Theor. Chem. Acc. **99**, 95 (1998)]. The total energies of all these species were refined by CCSD(T)/cc-pVTZ single-point calculations. The obtained potential energy surface has been used to outline the full kinetic scheme for the unimolecular decay of ion **1**. The rate constants of the various elementary steps have been calculated by the PST and the RRKM theory. We used a nonadiabatic version of the latter to evaluate the rate constants of the elementary steps which involve a change in the total spin multiplicity. We found that the two kinetically favored decomposition channels are the loss of atomic hydrogen, with formation of  $^2\text{CH}_2\text{S}^+$ , and molecular hydrogen, with formation of  $^1\text{HCS}^+$ . The former process is predicted to prevail for ions **1** in the lowest rotational states and with an internal energy content of at least 60 kcal mol<sup>-1</sup>. The loss of  $\text{H}_2$  was found to be by far the prevailing process in the time scale of ca. 10<sup>-5</sup> to ca. 10<sup>-6</sup> s from the formation of **1**. This is fully consistent with the experimentally observed exclusive loss of  $\text{H}_2$  by the  $\text{CH}_3\text{S}^+$  ions which decompose in the “metastable” time window of the mass spectrometer. The loss of  $\text{H}_2$  from ion **1** with formation of  $^1\text{HCS}^+$  may occur by two distinct “spin-forbidden” paths, i.e., a simple concerted 1,1  $\text{H}_2$  elimination or a 1,2 H shift followed by a 1,2  $\text{H}_2$  elimination from the singlet mercaptomethyl ion **2**. In the metastable time window, these two mechanisms may occur alternatively, depending on the degree of rotational excitation of **1**. © 1999 American Institute of Physics. [S0021-9606(99)30237-3]

## I. INTRODUCTION

The structure, stability, and thermochemistry of the thiomethoxy cation ( $\text{CH}_3\text{S}^+$ , **1**), and the mercapto-methyl cation ( $\text{CH}_2\text{SH}^+$ , **2**), as well as their unimolecular decomposition processes, have been intensively investigated over the last three decades.<sup>1</sup> Very accurate experiments<sup>1i</sup> as well as high level of theory *ab initio* calculations<sup>1i-n</sup> have firmly established that singlet **2** ( $^1A'$ ) is more stable than triplet **1** ( $^3A_1$ ) by ca. 30 kcal mol<sup>-1</sup>. In addition, it is well known<sup>1b-d</sup> that in the microsecond time scale typical of the mass spectrometric experiments, both of these ions undergo exclusively the unimolecular loss of  $\text{H}_2$ . The kinetic energy releases (KER) of the reactions



are essentially the same and measured as large as ca. 0.93 eV. For reaction (1), this finding is consistent with its interpretation<sup>1b</sup> in terms of a symmetry-forbidden 1,2 elimination which occurs adiabatically on the singlet  $A'$  potential energy surface. The mechanism of (2) is instead much less understood and its observed KER has not yet been clearly interpreted. The alternative explanations offered so far,<sup>1c</sup> including the isomerization of  $\text{CH}_3\text{S}^+$  to  $\text{CH}_2\text{SH}^+$  or to any alternative structure (common to  $\text{CH}_2\text{SH}^+$ ) prior to fragmentation, suffer from the scarce perception that reaction (2) is in fact a *spin-forbidden* process, which does not occur on a single potential energy surface. Therefore, even to achieve a qualitative description of its mechanism, one has to address aspects which are not easily tractable in the framework of the Born–Oppenheimer nonrelativistic quantum chemistry.<sup>2</sup> A recent study<sup>3</sup> has shown that the unimolecular loss of  $\text{H}_2$  from the strictly related methoxy cation,  $^3\text{CH}_3\text{O}^+$ , can occur, at least in principle, by two alternative paths:<sup>4</sup>



<sup>a)</sup>Present address: Dipartimento di Chimica, Università di Roma, “La Sapienza”, P. le Aldo Moro, 5, DO185 Rome, Italy.

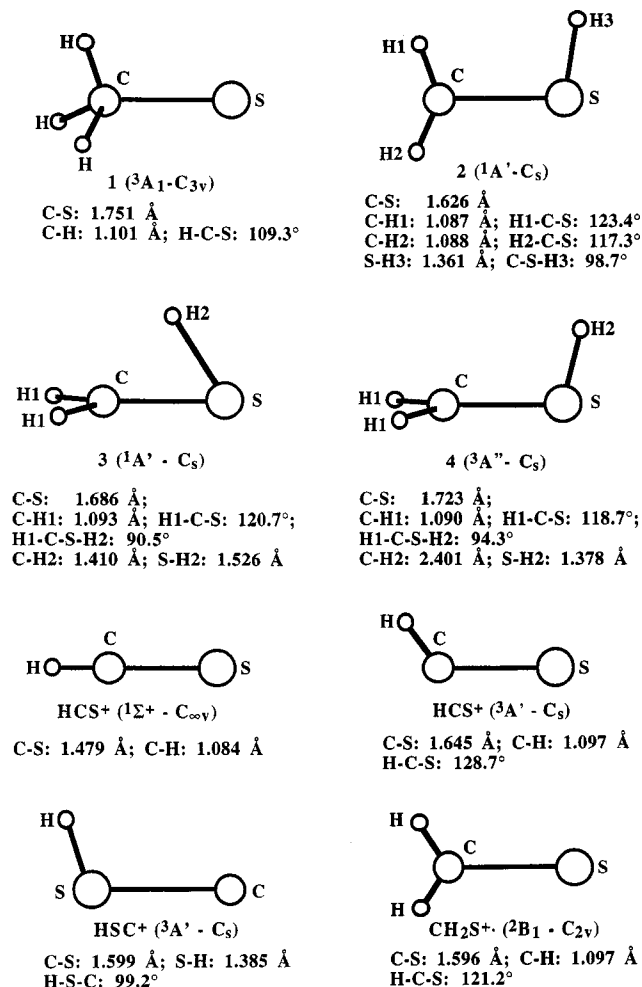


FIG. 1. B3LYP/6-311+G(*d,p*) optimized geometries of the  $[C,H_3,S]^+$  isomers and their fragments.

i.e., a concerted nonadiabatic 1,1 H<sub>2</sub> elimination or a stepwise mechanism, consisting of a nonadiabatic 1,2 H shift followed by an adiabatic H<sub>2</sub> elimination. The same competition between the two channels



as well as alternative decomposition routes are in principle conceivable for the thiomethoxy cation. In addition, we cannot rule out that in a time interval different from the microsecond, ions **1** may undergo unimolecular decompositions different from (2) with formation of products other than H<sub>2</sub>. Therefore, we decided to perform density functional theory (DFT), *ab initio*, and Phase-space/Rice Ramsperger Kassel Marcus (PST/RRKM) calculations to investigate the mechanism of the unimolecular decay of the thiomethoxy cation. The results of this study will be discussed in the present article.

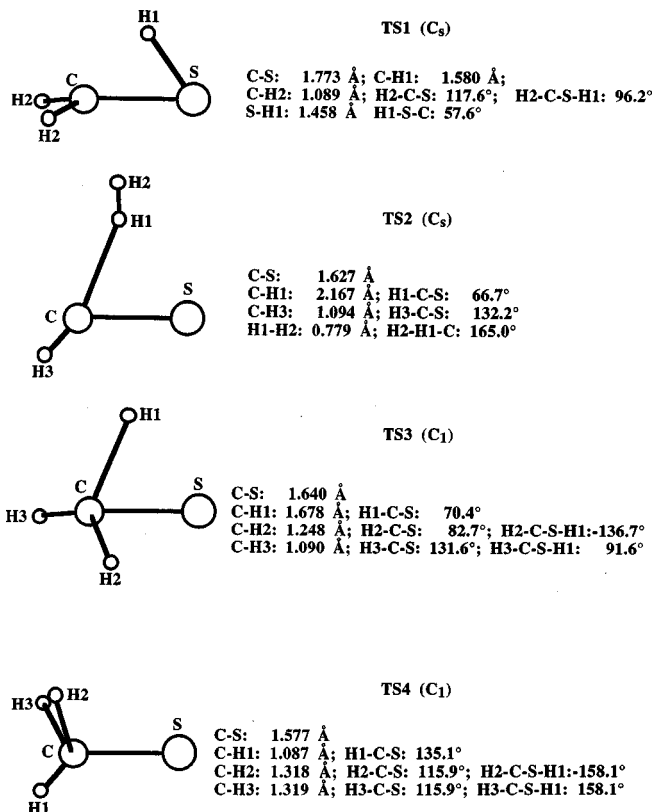


FIG. 2. B3LYP/6-311+G(*d,p*) optimized geometries of the  $[C,H_3,S]^+$  transition structures.

## II. THEORETICAL METHODS

### A. Location of the critical points on the adiabatic surfaces

The geometries of all the minima and the transition structures lying on the singlet and triplet  $[C,H_3,S]^+$  potential energy surfaces and conceivably involved in the unimolecular decomposition of the thiomethoxy cation were optimized, within the specified symmetry constraints, at the density functional level of theory (DFT) using the hybrid B3LYP functional<sup>5</sup> and the 6-311+G(*d,p*) basis set.<sup>6</sup> The located

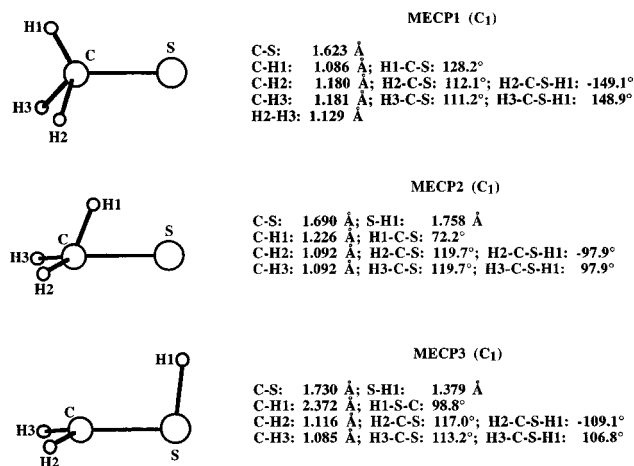


FIG. 3. B3LYP/6-311+G(*d,p*) optimized geometries of the  $[C,H_3,S]^+$  minimum energy crossing points.

TABLE I. Total energies (hartrees), zero-point energies (hartrees), and relative energies (kcal mol<sup>-1</sup>) of the [C,H<sub>3</sub>,S]<sup>+</sup> ions and their fragments.

Species	B3LYP/B1 <sup>a</sup>	CCSD(T)/B2 <sup>b,c</sup>	ZPE <sup>c</sup>	ΔE <sup>d</sup>
<b>1</b> ( <sup>3</sup> A <sub>1</sub> )	-437.760 10	-437.191 16	0.035 05	0
<b>2</b> ( <sup>1</sup> A')	-437.801 80	-437.236 71	0.035 03	-28
<b>3</b> ( <sup>1</sup> A')	-437.722 71	-437.157 73	0.030 81	+18
<b>4</b> ( <sup>3</sup> A'')	-437.713 98	-437.143 31	0.030 63	+27
<b>TS1</b> ( <sup>3</sup> A'')	-437.681 26	-437.110 71	0.028 60	+46
<b>TS2</b> ( <sup>3</sup> A')	-437.618 69	-437.045 48	0.022 68	+84
<b>TS3</b> ( <sup>1</sup> A)	-437.710 42	-437.143 04	0.031 88	+28
<b>TS4</b> ( <sup>1</sup> A)	-437.698 32	-437.131 07	0.028 71	+34
<b>MECP1</b>	-437.702 50	-437.134 60	0.029 82	+32
<b>MECP2</b>	-437.719 55	-437.153 40	0.031 40	+21
<b>MECP3</b>	-437.712 10		0.034 29	+30 <sup>e</sup>
<b>HCS<sup>+</sup></b> ( <sup>1</sup> Σ <sup>+</sup> )	-436.558 45	-436.005 33	0.014 36	
				+2
<b>H<sub>2</sub></b> ( <sup>1</sup> Σ <sub>g</sub> <sup>+</sup> )	-1.179 57	-1.172 33	0.010 07	
<b>CH<sub>2</sub>S<sup>+</sup></b> ( <sup>2</sup> B <sub>2</sub> )	-437.159 05	-436.593 97	0.023 65	
				+54
<b>H</b> ( <sup>2</sup> S)	-0.502 16	-0.499 81		
<b>CH<sub>3</sub><sup>+</sup></b> ( <sup>1</sup> A' <sub>1</sub> )	-39.491 39	-39.404 38	0.031 16	
				+81
<b>S</b> ( <sup>3</sup> P)	-398.133 07	-397.653 35		
<b>HCS<sup>+</sup></b> ( <sup>3</sup> A')	-436.430 70	-435.871 47	0.011 25	
<b>HSC<sup>+</sup></b> ( <sup>3</sup> A')	-436.384 55	-435.829 08	0.009 92	

<sup>a</sup>B1=6-311+G(d,p).<sup>b</sup>B2=cc-pVTZ.<sup>c</sup>At the B3LYP/B1 optimized geometries.<sup>d</sup>CCSD(T)/B2 relative energies at 0 K.<sup>e</sup>B3LYP/B1 relative energy at 0 K.

critical points were subsequently characterized by computing their B3LYP/6-311+G(d,p) analytical second derivatives and their total energies were refined by performing single-point calculations at the coupled-cluster level of theory, including the effect of connected triples, CCSD(T).<sup>7</sup> To this end, we used the correlation-consistent polarized valence basis set of triple-zeta quality developed by Dunning (cc-pVTZ).<sup>8</sup> Thermal corrections were computed according to standard statistical mechanics formulas<sup>9</sup> using the B3LYP/6-311+G(d,p) moments of inertia and unscaled

TABLE III. CCSD(T)/cc-pVTZ//B3LYP/6-311+G(d,p) and experimental<sup>a</sup> enthalpy changes (298 K, kcal mol<sup>-1</sup>) of decomposition reactions involving the [C,H<sub>3</sub>,S]<sup>+</sup> ions.

Reaction	Calculated	Experimental
<sup>1</sup> CH <sub>2</sub> SH <sup>+</sup> → <sup>1</sup> HCS <sup>+</sup> + H <sub>2</sub>	+32	+31.5
<sup>3</sup> CH <sub>3</sub> S <sup>+</sup> → <sup>1</sup> HCS <sup>+</sup> + H <sub>2</sub>	+3	-2
<sup>3</sup> CH <sub>3</sub> S <sup>+</sup> → <sup>2</sup> CH <sub>2</sub> S <sup>+</sup> + H	+54	+52.6

<sup>a</sup>The enthalpies of formation of <sup>1</sup>CH<sub>2</sub>SH<sup>+</sup>, 211.5 kcal mol<sup>-1</sup>, <sup>3</sup>CH<sub>3</sub>S<sup>+</sup>, 245 kcal mol<sup>-1</sup>, and <sup>2</sup>CH<sub>2</sub>S<sup>+</sup>, 246 kcal mol<sup>-1</sup>, are taken from Ref. 1i. The enthalpies of formation of <sup>1</sup>HCS<sup>+</sup>, 243 kcal mol<sup>-1</sup>, and H, 51.6 kcal mol<sup>-1</sup>, are taken from S. G. Lias, J. A. Bartmess, J. F. Liebman, J. L. Holmes, R. D. Levin, and W. G. Mallard, J. Phys. Chem. Ref. Data Suppl. **1**, 17 (1988).

harmonic frequencies. All these calculations have been performed using the GAUSSIAN 94 set of programs.<sup>10</sup>

## B. Location and characterization of the crossing points

The critical points lying on the hyperline of intersection<sup>11</sup> between the singlet and triplet [C,H<sub>3</sub>,S]<sup>+</sup> potential energy surfaces were located at the B3LYP/6-311+G(d,p) level of theory using a recently described steepest descent-based method.<sup>12</sup> Some of these points were also refined at the CCSD(T)/cc-pVTZ//B3LYP/6-311+G(d,p) hybrid level<sup>12</sup> using the B3LYP gradients and the CCSD(T) electronic energies. The crossing points located at the B3LYP/6-311+G(d,p) level of theory were approximately ascertained to be minima along the 3N-7 dimensional crossing hyperline (MECPs) by verifying the absence of negative eigenvalues in the corresponding effective Hessian matrix.<sup>12</sup> The harmonic frequencies at the crossing points needed for the kinetic calculations described below were also obtained in this way.

For all the located MECPs, we evaluated the spin-orbit coupling (SOC) matrix elements, known to drive the inter-system crossing in the vicinity of the crossing point,<sup>2a</sup> between the singlet and the three substates of the triplet using

TABLE II. B3LYP/6-311+G(d,p) vibrational harmonic frequencies (cm<sup>-1</sup>) and rotational constants (GHz) of the [C,H<sub>3</sub>,S]<sup>+</sup> ions and their fragments.

Species	Vibrational frequencies									Rotational constants		
	734	837	838	1316	1337	1337	2942	3023	3023	155.0	14.0	14.0
<b>1</b> ( <sup>3</sup> A <sub>1</sub> )	734	837	838	1316	1337	1337	2942	3023	3023	155.0	14.0	14.0
<b>2</b> ( <sup>1</sup> A')	853	865	1033	1069	1128	1470	2595	3121	3241	143.4	17.2	15.3
<b>3</b> ( <sup>1</sup> A')	234	463	956	1001	1193	1477	1966	3058	3177	158.0	15.0	15.0
<b>4</b> ( <sup>3</sup> A'')	412	632	760	783	874	1308	2436	3056	3185	140.0	14.4	14.7
<b>TS1</b> ( <sup>3</sup> A'')	1515i	583	736	771	811	1304	2081	3062	3206	149.0	14.2	14.3
<b>TS2</b> ( <sup>3</sup> A')	375i	98	155	421	523	830	1076	3113	3740	13.0	18.8	42.2
<b>TS3</b> ( <sup>1</sup> A)	443i	781	973	1027	1145	1418	2694	2786	3169	14.6	14.9	156.0
<b>TS4</b> ( <sup>1</sup> A)	873i	590	841	902	1132	1501	1575	2878	3181	15.0	16.1	157.0
<b>MECP1</b>		449	896	1078	1080	1468	2390	2547	3181	15.0	15.9	164.2
<b>MECP2</b>		898	927	999	1212	1456	2074	3051	3168	15.1	15.3	159.7
<b>MECP3</b>		550	643	999	1190	2424	2845	3144	3255	14.6	14.7	136.0
<b>HCS<sup>+</sup></b> ( <sup>1</sup> Σ <sup>+</sup> )	792	792	1456	3263						21.3		
<b>HCS<sup>+</sup></b> ( <sup>3</sup> A')	796	1057	3087							18.2	18.6	806.0
<b>HSC<sup>+</sup></b> ( <sup>3</sup> A')	927	1050	2377							20.6	22.2	280.0
<b>CH<sub>2</sub>S<sup>+</sup></b> ( <sup>2</sup> B <sub>2</sub> )	798	1010	1064	1379	3016	3116				17.0	18.0	285.0
<b>CH<sub>3</sub><sup>+</sup></b> ( <sup>1</sup> A' <sub>1</sub> )	1406	1406	1418	3019	3214	3214				140.0	279.0	279.0
<b>H<sub>2</sub></b> ( <sup>1</sup> Σ <sub>g</sub> <sup>+</sup> )	4419									1810.9		

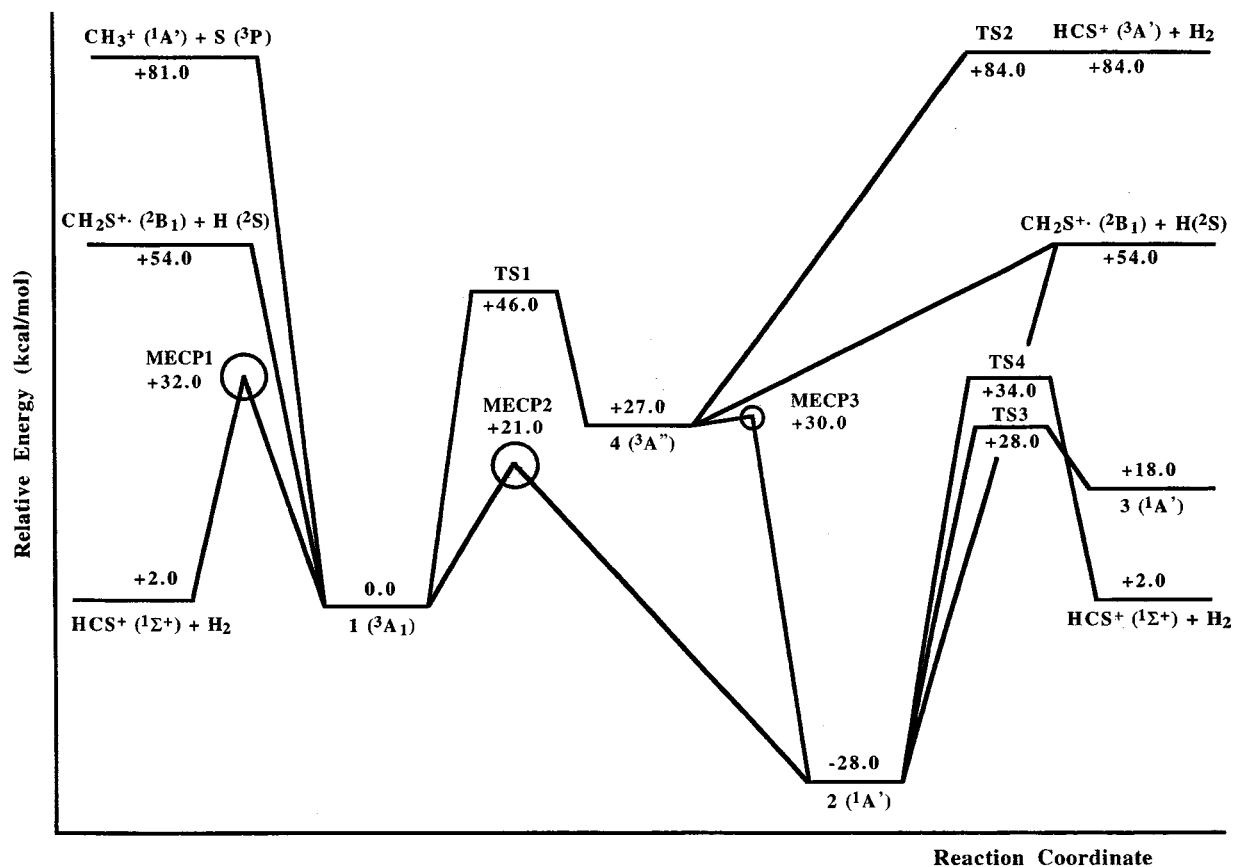


FIG. 4. CCSD(T)/cc-pVTZ//B3LYP/6-311+G(*d,p*) potential energy diagram (0 K) of the  $[C,H_3,S]^+$  isomers and their interconnecting structures and dissociation products.

first order CI wavefunctions developed in the singlet RHF/VTZ orbitals (practically the same results were obtained using wavefunctions developed in the triplet ROHF/cc-pVTZ orbitals). To this end, we employed the one electron approximate spin-orbit Hamiltonian

$$H_{so} = (\alpha^2/r) \sum Z_a^{\text{eff}} (1/r_{ia}^3) (\mathbf{r}_{ia} \times \mathbf{p}_i) \mathbf{s}_i,$$

implemented in the GAMESS96 program,<sup>13</sup> using values of the effective nuclear charges ( $Z_a^{\text{eff}}$ ) recommended in the literature.<sup>14</sup>

### C. Calculation of the rate constants

Based on the characteristics<sup>15</sup> of the elementary steps involved in the unimolecular decay of  $CH_3S^+$  (*vide infra*), we have calculated the corresponding microscopic rate constants at internal energy  $E$  and angular momentum  $J$  of the reactant species using the transition state theory in its different formulations.

The rate constants of adiabatic reactions which involve a ‘‘tight’’ transition state (TS) were calculated according to the expression based on the RRKM theory<sup>15</sup>

$$k_i(E, J) = [1/h\rho(E, J)] \int \kappa(E') \rho^\#(E - E' - E^\#, J) dE'.$$

Here  $\rho^\#(E, J)$  and  $\rho(E, J)$  are the densities of the vibrational states at the TS and at the minimum, respectively, and  $\kappa(E')$

is the transmission coefficient for the tunneling correction. This term was calculated using the formula outlined by Miller<sup>16</sup> for a generalized Eckart potential

$$\kappa(E) = \sinh(a) \sinh(b) / [\sinh^2(0.5a + 0.5b) + \cosh^2(c)],$$

where

$$a = (4\pi/h\nu^\#)(E + V_0)^{1/2}(V_0^{-1/2} + V_1^{-1/2})^{-1},$$

$$b = (4\pi/h\nu^\#)(E + V_1)^{1/2}(V_0^{-1/2} + V_1^{-1/2})^{-1},$$

$$c = 2\pi[V_0V_1/(h\nu^\#)^2 - 1/16]^{1/2},$$

$V_1 - V_0$  being the energy change of the reaction (excluding the zero-point energies) and  $\nu^\#$  the value of the imaginary frequency.

The rate constants of barrier-free (loose TS) adiabatic reactions were calculated according to the equation based on the Phase-space theory (PST)<sup>17</sup>

$$k_i(E, J) = [1/h\rho(E, J)] S \int \rho^\#(E - E_{tr} - E^\#, J) \Gamma(E_{tr}, J) dE_{tr},$$

where  $S$  is the symmetry number ratio,  $E_{tr}$  is the product translational energy sum, and  $\Gamma$  is the rotational-orbital sum of the states function.<sup>15b,17</sup> We note here that the rate constants calculated according to phase space theory can in some cases slightly overestimate the real values.<sup>17d,e</sup>

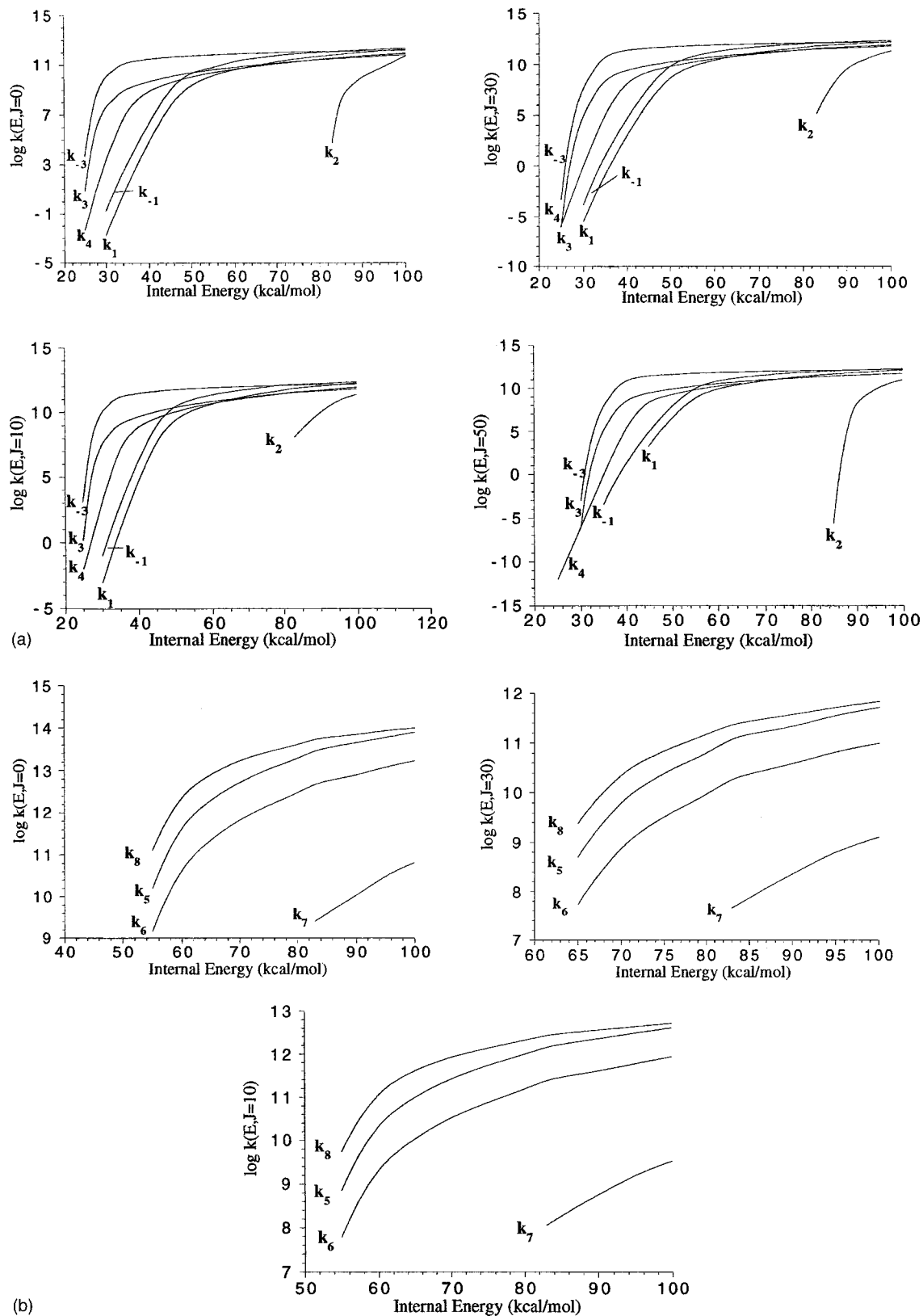


FIG. 5. (a) Calculated rate constants of the elementary steps reported in Chart I which involve a tight transition structure. (b) Calculated rate constants of the elementary steps reported in Chart I which involve a loose transition structure. (c) Calculated rate constants of the nonadiabatic elementary steps reported in Chart I.

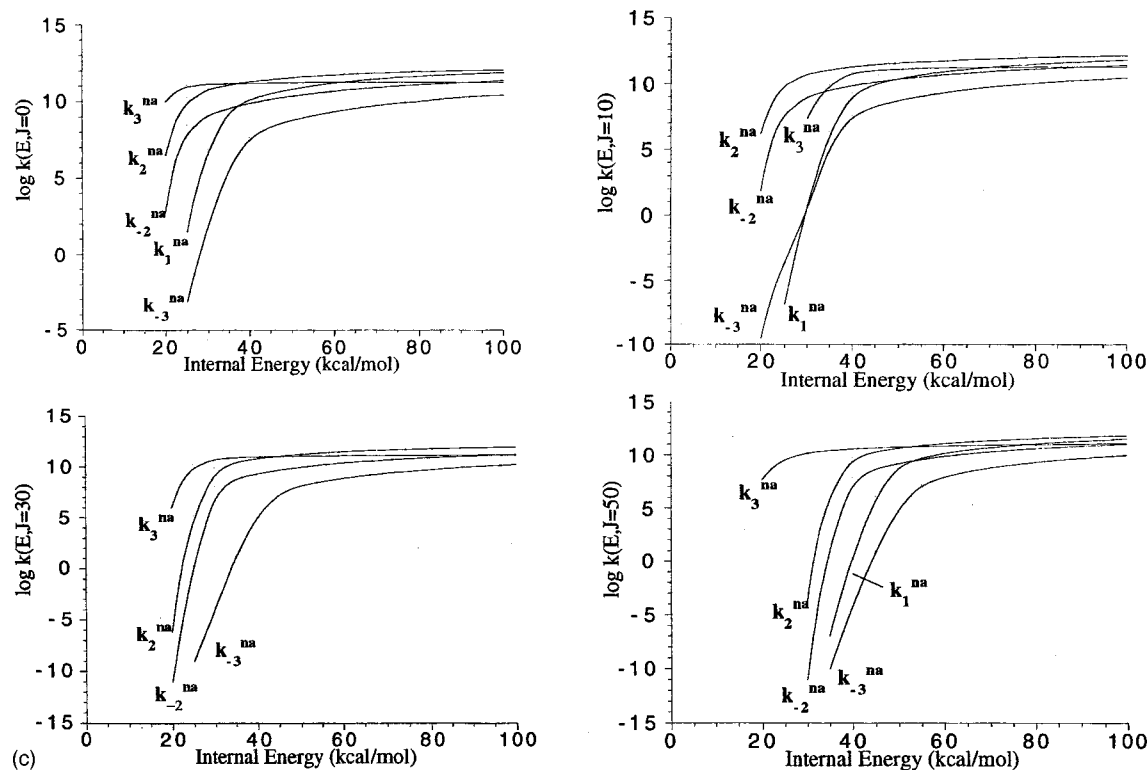


FIG. 5. (Continued.)

All these calculations were performed using a FORTRAN90 routine written by the authors and based on the steepest-descent algorithm<sup>18</sup> for the calculation of the density of the vibrational states, and employing a Langevin-type potential<sup>15b</sup> to describe the interaction of the dissociating fragments. The nonadiabatic (na) rate constants of reactions which occur by surface hopping were calculated using the expression based on a nonadiabatic version of the RRKM theory<sup>19</sup>

$$k_i^{\text{na}}(E, J) = [1/h\rho(E, J)] \int \rho^{\text{MECP}}(E_u, J) \times p(E - E_u - E_c, J) dE_u,$$

where  $\rho^{\text{MECP}}$  is the density of the states at the MECP calculated using the corresponding frequencies,  $E_c$  is the energy of the MECP with respect to the minimum, and  $p(E - E_u - E_c, J)$  is the transition probability calculated when the internal energy of the complex in the  $J$  rotational state is equal to  $(E - E_u)$ .

These calculations were performed using a FORTRAN90 program<sup>20</sup> which calculates the term  $p(E)$  according to a formula developed by Delos and Thorson.<sup>21</sup> It is based on a one-dimensional model which takes into account the tunneling probability and which coincides with the Landau-Zener formula for large values of the internal energy

$$p(E) = 4\pi^2 H_{\text{so}} [2\mu/h^2 F(F_1 - F_2)]^{2/3} \times \text{Ai}^2[-E(2\mu(F_1 - F_2)/h^2 F^4)]^{1/3}.$$

Here Ai is the Airy function<sup>22</sup> and  $\mu$ ,  $F_1 - F_2$ , and  $F$  are the effective mass, the difference, and the geometric mean of the

gradients, respectively, at the MECs. All these calculations were performed using the CCSD(T)/cc-pVTZ//B3LYP/6-311+G( $d,p$ ) electronic energies and the B3LYP/6-311+G( $d,p$ ) rotational constants and unscaled harmonic frequencies.

### III. RESULTS

#### A. Outline of the potential energy surface

The B3LYP/6-311+G( $d,p$ ) optimized geometries of all the presently investigated  $[\text{C}_2\text{H}_3\text{S}]^+$  ions and their fragments are shown in Figs. 1, 2, and 3, and their absolute and relative energies, and harmonic frequencies and moments of inertia, are collected in Tables I and II, respectively. We have also reported in Table III the presently computed CCSD(T)/cc-pVTZ//B3LYP/6-311+G( $d,p$ ) enthalpy changes of selected reactions involving the  $[\text{C}_2\text{H}_3\text{S}]^+$  ions and the corresponding experimental values. The comparison between the two sets of data suggests that the CCSD(T)/cc-pVTZ//B3LYP/6-311+G( $d,p$ ) energy differences between the various  $[\text{C}_2\text{H}_3\text{S}]^+$  ions, diagrammatically shown in Fig. 4, should be as accurate as few kilocalories per mol. Consistent with the results of previous theoretical studies,<sup>1e,i-n</sup> the mercaptomethyl cation **2** was found to be the absolute minimum on the singlet surface. It is more stable than the bridged structure **3** by 46 kcal mol<sup>-1</sup>, and their interconversion through the transition structure **TS3** requires 56 kcal mol<sup>-1</sup> with respect to **2**. The energy change for the

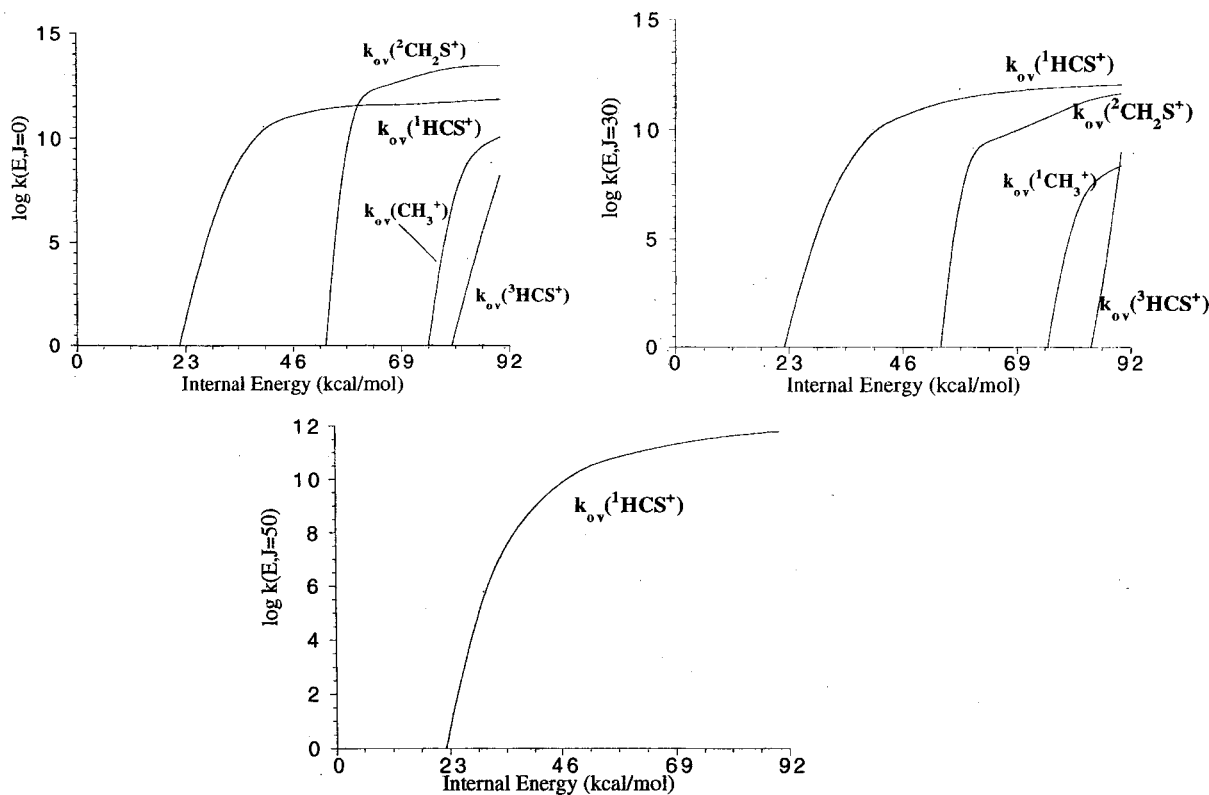


FIG. 6. Calculated overall rate constants for the formation of  $^1\text{HCS}^+$ ,  $^2\text{CH}_2\text{S}^+$ ,  $^1\text{CH}_3^+$ , and  $^3\text{HCS}^+$  from ion **1**.

loss of atomic hydrogen from isomer **2** is as large as  $82 \text{ kcal mol}^{-1}$  and involves a practically negligible energy barrier. Instead, the loss of  $\text{H}_2$  from **2** with formation of  $\text{HCS}^+(^1\Sigma^+)$  requires to overcome the energy barrier of  $62 \text{ kcal mol}^{-1}$  corresponding to the transition structure **TS4**. The thiomethoxy cation **1** is the absolute minimum on the triplet surface. It is more stable than the triplet mercaptomethyl cation **4** by  $27 \text{ kcal mol}^{-1}$ , and the two isomers are separated by an energy barrier of  $46 \text{ kcal mol}^{-1}$  with respect to **1**. The loss of atomic hydrogen from both isomers **1** and **4** was found to be practically barrier-free and requires  $54$  and  $27 \text{ kcal mol}^{-1}$ , respectively. In addition, the loss of  $\text{H}_2$  from **4** with formation of  $\text{HCS}^+(^3A')$  requires to overcome the energy barrier of  $84 \text{ kcal mol}^{-1}$  corresponding to the transition structure **TS2**. The triplet isomer **1** is less stable than the singlet isomer **2** by  $28 \text{ kcal mol}^{-1}$ . The latter species is therefore the most stable among the various singlet and triplet  $[\text{C},\text{H}_3,\text{S}]^+$  isomers.

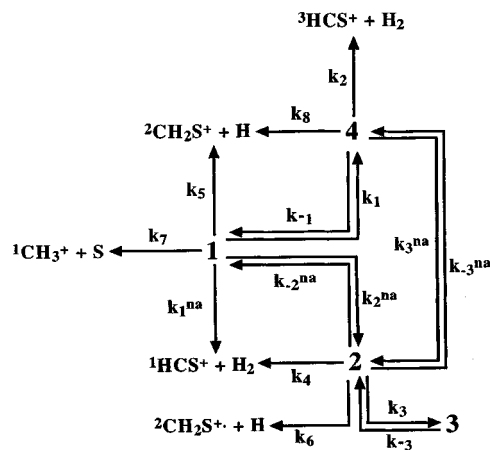
Searching for the crossing points between the investigated regions of the singlet and triplet  $[\text{C},\text{H}_3,\text{S}]^+$  potential energy surfaces leads to the location of three distinct MECPs. The reaction paths corresponding to these structures have been ascertained using an approximate (Intrinsic Reaction Coordinate (IRC) procedure<sup>23</sup> which showed that **MECP1** allows the  $1,1 \text{ H}_2$  elimination from triplet **1** with formation of  $\text{HCS}^+(^1\Sigma^+)$  and  $\text{H}_2$ , **MECP2** interconnects isomers **1** and **2** through a  $1,2 \text{ H}$  migration, and **MECP3** leads to the interconversion of the mercaptomethyl structures **2** and **4**. The corresponding SOC magnitudes, expressed as the root mean-square of the matrix elements between the

singlet and the three substates of the triplet, were computed as  $221$ ,  $252$ , and  $120 \text{ cm}^{-1}$ .

## B. Calculation of the rate constants

The potential energy diagram shown in Fig. 4 has been used to outline the kinetic scheme depicted in Chart I. All the involved rate constants have been calculated by varying the internal energy of the reactant ion, referred to

Chart I



**1**, from  $0$  to  $100 \text{ kcal mol}^{-1}$ , and the calculation has been repeated for selected values of the  $J$  quantum number, including  $0$ ,  $10$ ,  $30$ ,  $50$ , and  $100$ . The rate constants  $k_1$ ,  $k_{-1}$ ,  $k_2$ ,  $k_3$ ,  $k_{-3}$ , and  $k_4$ , which involve a ‘tight’ tran-

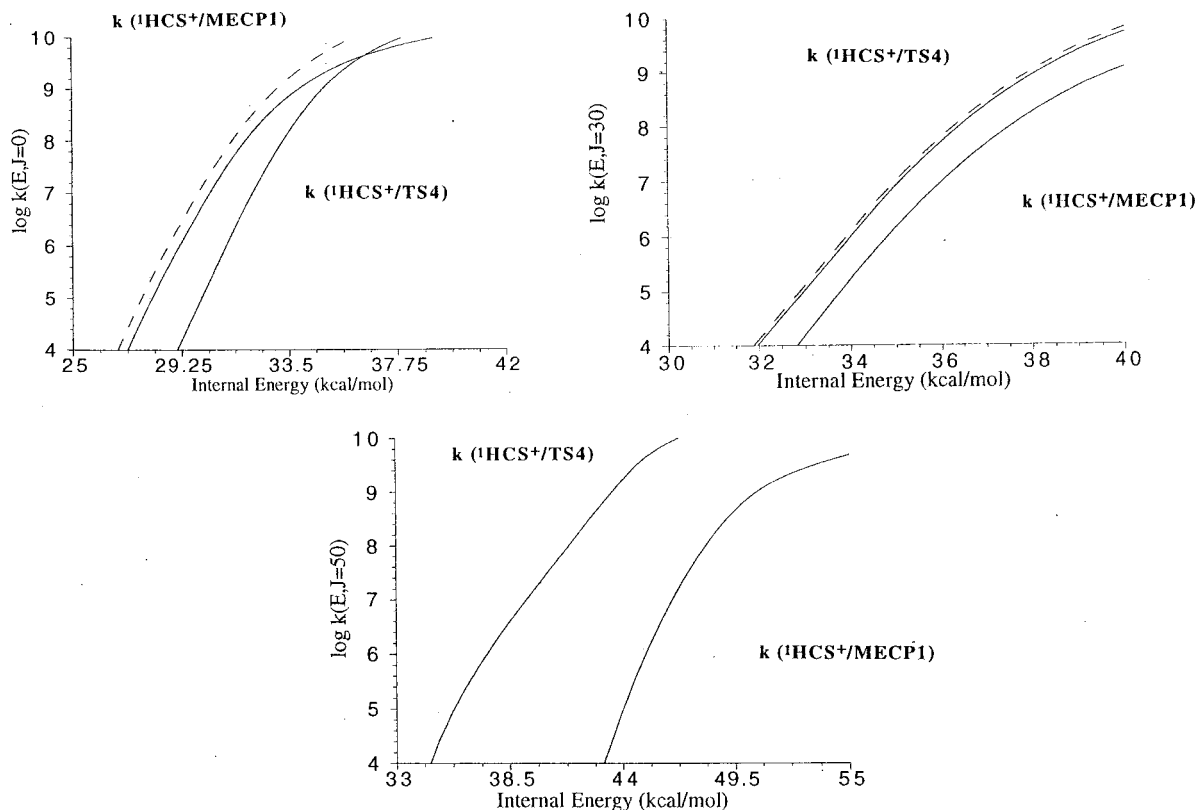


FIG. 7. Calculated overall rate constants (dotted lines) for the formation of  ${}^1\text{HCS}^+$  from ion **1**. They are the sum of  $k({}^1\text{HCS}^+/\text{MECP1})$  and  $k({}^1\text{HCS}^+/\text{TS4})$ .

sition structure, have been calculated according to the RRKM theory and their  $(E, J)$  dependence is shown in Fig. 5(a). Figure 5(b) shows the  $(E, J)$  dependence of the rate constants  $k_5$ ,  $k_6$ ,  $k_7$ , and  $k_8$ , which involve a ‘‘loose’’ transition structure and have been calculated according to the PST theory, and Fig. 5(c) shows the  $(E, J)$  dependence of the nonadiabatic rate constants, calculated using a nonadiabatic version of the RRKM theory. In these figures, we have not included the rate constants whose calculated values resulted to be lower than  $10^{-10} \text{ s}^{-1}$ .<sup>24</sup>

#### IV. DISCUSSION

We are now in the position to discuss the detailed mechanism of the unimolecular decay of the thiomethoxy cation,  $\text{CH}_3\text{S}^+$ . According to the kinetic scheme depicted in Chart I, this species may in principle undergo a number of alternative decomposition routes, eventually leading to the four ionic products  ${}^1\text{HCS}^+$ ,  ${}^2\text{CH}_2\text{S}^+$ ,  ${}^3\text{HCS}^+$ , and  ${}^1\text{CH}_3^+$ .

Using the steady-state approximation, the phenomenological rate constants corresponding to the formation of these products,  $k_{\text{ov}}(P_i^+)$  ( $P_i^+ = {}^1\text{HCS}^+$ ,  ${}^2\text{CH}_2\text{S}^+$ ,  ${}^3\text{HCS}^+$ , and  ${}^1\text{CH}_3^+$ ),

$$d[{}^1\text{HCS}^+]/dt = k_{\text{ov}}({}^1\text{HCS}^+)[\text{CH}_3\text{S}^+],$$

$$d[{}^2\text{CH}_2\text{S}^+]/dt = k_{\text{ov}}({}^2\text{CH}_2\text{S}^+)[\text{CH}_3\text{S}^+],$$

$$d[{}^1\text{CH}_3^+]/dt = k_{\text{ov}}({}^1\text{CH}_3^+)[\text{CH}_3\text{S}^+],$$

$$d[{}^3\text{HCS}^+]/dt = k_{\text{ov}}({}^3\text{HCS}^+)[\text{CH}_3\text{S}^+],$$

are expressed as follows:

$$k_{\text{ov}}({}^1\text{HCS}^+) = k_1^{\text{na}} + [k_4 A_3 / (k_4 + k_6 + k_{-2}^{\text{na}} + k_{-3}^{\text{na}})],$$

$$k_{\text{ov}}({}^2\text{CH}_2\text{S}^+) = [k_6 / (k_4 + k_6 + k_{-2}^{\text{na}} + k_{-3}^{\text{na}})] A_3 + k_5 + k_8 (A_1 / A_2),$$

$$k_{\text{ov}}({}^1\text{CH}_3^+) = k_7,$$

$$k_{\text{ov}}({}^3\text{HCS}^+) = k_2 (A_1 / A_2),$$

where

$$A_1 = k_1 + (k_3^{\text{na}} k_{-3}^{\text{na}}) / (k_4 + k_6 + k_{-2}^{\text{na}} + k_{-3}^{\text{na}}),$$

$$A_2 = k_2 + k_8 + k_3^{\text{na}} + k_{-1} - (k_3^{\text{na}} k_{-3}^{\text{na}}) / (k_4 + k_6 + k_{-2}^{\text{na}} + k_{-3}^{\text{na}}),$$

$$A_3 = k_2^{\text{na}} + k_3^{\text{na}} (A_1 / A_2).$$

The values of  $k_{\text{ov}}(P_i^+)$  have been calculated for different values of internal energy and angular momentum of the  $\text{CH}_3\text{S}^+$  ion **1**. The resulting curves, depicted in Fig. 6, furnish the following indications. For  $J=50$ , the overall reaction corresponding to the formation of the thermochemically most stable products  ${}^1\text{HCS}^+$  and  $\text{H}_2$  is by far the most efficient one. For  $J=30$  and internal energies of **1** up to ca. 70 kcal mol<sup>-1</sup>,  $k_{\text{ov}}({}^1\text{HCS}^+)$  is again significantly larger than the other three overall constants. However, for  $J=30$  and for the highest sampled internal energies of **1**, the rate constants  $k_{\text{ov}}({}^1\text{HCS}^+)$  and  $k_{\text{ov}}({}^2\text{CH}_2\text{S}^+)$  tend to become comparable.

Therefore, for  $J=30$  and high internal energies, ions **1** are expected to undergo the loss of atomic and molecular hydrogen at a comparable extent. For  $J=0$ , the loss of atomic hydrogen is instead expected to prevail for internal energies of **1** larger than ca. 60 kcal mol<sup>-1</sup>. However, up to this value of internal energy, ions **1** are expected to undergo exclusively the loss of  $\text{H}_2$ . As mentioned in the introduction, the unimolecular decomposition processes of **1** experimentally observed to date are those which occur in the “metastable” time window of the mass spectrometers. It means that the sampled  $\text{CH}_3\text{S}^+$  ions are those which decompose in approximately  $10^{-6}$  to  $10^{-5}$  s from their formation in the ion source. Consistent with the experimental observation of the exclusive occurrence of reaction (2) with formation of  $\text{H}_2$ , we note from Fig. 6 that, irrespective of the  $J$  quantum number, the only unimolecular reaction which can occur at a rate constant of ca.  $10^5$  to  $10^6$  s<sup>-1</sup> is in fact the loss of  $\text{H}_2$ . We decided to focus greater attention on the mechanistic details of this process. According to the kinetic scheme of Chart I, taking into account the negligible value of  $k_1$  with respect to  $k_1^{\text{na}}$  and  $k_2^{\text{na}}$ , the loss of  $\text{H}_2$  from **1** may in practice occur by two alternative paths. The first one passes through **MECP1** and is a simple concerted 1,1  $\text{H}_2$  elimination. The second eventually passes through **TS4** and is a 1,2 H shift followed by a 1,2  $\text{H}_2$  elimination from the singlet mercaptomethyl ion **2**. The corresponding rate constants  $k(^1\text{HCS}^+/\text{MECP1})$  and  $k(^1\text{HCS}^+/\text{TS4})$  can be expressed as follows:

$$k(^1\text{HCS}^+/\text{MECP1}) = k_1^{\text{na}},$$

$$k(^1\text{HCS}^+/\text{TS4}) = k_2^{\text{na}}k_4/(k_4 + k_{-2}^{\text{na}}).$$

The overall rate constant for the formation of  $^1\text{HCS}^+$ , which is just the sum of these two terms, has been calculated for different values of the internal energy and angular momentum of **1**. The obtained values are depicted in Fig 7, which, for the reason of clarity, also shows the trends of the two above contributing terms. For the lowest sampled degree of rotational excitation of **1**, i.e.,  $J=0$ , and for its lowest internal energies,  $k(^1\text{HCS}^+/\text{MECP1})$  is by far the prevailing contribution to the overall rate constant for the formation of  $^1\text{HCS}^+$ . Therefore, in the metastable time window, the mechanism of reaction (2) can be safely described in terms of a simple nonadiabatic 1,1  $\text{H}_2$  elimination. This is the consequence of the relatively high contribution of tunneling to the rate constant  $k_1^{\text{na}}$ . For  $J=0$  and internal energies of **1** ranging around 35–40 kcal mol<sup>-1</sup>,  $k(^1\text{HCS}^+/\text{MECP1})$  and  $k(^1\text{HCS}^+/\text{TS4})$  become comparable and the mechanism of reaction (2) must be therefore perceived as the concomitant occurrence of a simple nonadiabatic 1,1  $\text{H}_2$  elimination and a 1,2 H shift followed by a 1,2  $\text{H}_2$  elimination from the singlet mercaptomethyl ion **2**. The latter mechanistic path becomes prevailing for  $J=0$  and the largest values of internal energies of **1**. The same holds true for  $J=30$  and  $J=50$ , irrespective of the internal energy of **1**.

The data reported in Fig. 7 are also in good agreement with the available information concerning the kinetic energy released in the unimolecular decomposition (2), experimentally measured as 0.93 eV. We can in fact observe from Fig.

7 that, depending on the assumed rotational degree of excitation, the ions **1** which undergo the unimolecular loss of  $\text{H}_2$  in a time of ca.  $10^{-6}$ – $10^{-5}$  s from their formation in the ion source are predicted to possess internal energies of ca. 28–38 kcal mol<sup>-1</sup>. Therefore, the experimentally observed KER amounts to ca. 60%–80% of the available internal energy of decomposing ions **1**. These high fractions are quite consistent with the usually high kinetic energy releases which are observed<sup>25</sup> in the decomposition of simple ions which produce biatomic and triatomic molecules and ions.

## V. CONCLUSIONS

Our computational study on the unimolecular decay of the triplet thiomethoxy cation **1** allows to draw the following concluding remarks. The two lowest-energy decomposition channels predicted for this ion are the loss of atomic hydrogen, with formation of  $^2\text{CH}_2\text{S}^+$ , and molecular hydrogen, with formation of  $^1\text{HCS}^+$ . The former process is found to be prevailing only for ions **1** in the lowest rotational states and high vibrational states, i.e., with an internal energy content of at least 60 kcal mol<sup>-1</sup>. The loss of  $\text{H}_2$  was found to be by far the prevailing decomposition process in the time scale of ca.  $10^{-5}$  to ca.  $10^{-6}$  s, which is consistent with the exclusive observation of the loss of  $\text{H}_2$  by the  $\text{CH}_3\text{S}^+$  ions observed to decompose in the “metastable” time window of the mass spectrometers. Generally speaking, the loss of  $\text{H}_2$  from ion **1** may occur by two distinct paths, i.e., a simple nonadiabatic concerted 1,1  $\text{H}_2$  elimination or a nonadiabatic 1,2 H shift followed by an adiabatic 1,2  $\text{H}_2$  elimination from the singlet mercaptomethyl ion **2**. In the metastable time window, these two mechanisms may occur alternatively, depending on the degree of internal and rotational excitation of ion **1**.

## ACKNOWLEDGMENTS

This work was financially supported by the Italian Ministero dell' Università e della Ricerca Scientifica e Tecnologica (MURST) and the Consiglio Nazionale delle Ricerche (CNR). We gratefully acknowledge stimulating discussions with Dr. Jeremy Harvey and Dr. Detlef Schröder.

- <sup>1</sup>(a) J. H. Beynon, A. E. Fontaine, and G. R. Lester, *Int. J. Mass Spectrom. Ion Phys.* **1**, 1 (1968); (b) D. H. Williams and G. Hvistendahl, *J. Am. Chem. Soc.* **96**, 6753 (1974); (c) A. G. Harrison, *ibid.* **100**, 4911 (1978); (d) J. D. Dill and F. W. McLafferty, *ibid.* **101**, 6526 (1979); (e) M. J. S. Dewar and H. S. Rzepa, *ibid.* **99**, 7432 (1977); (f) R. E. Kutina, A. K. Edwards, G. L. Goodman, and J. Berkowitz, *J. Chem. Phys.* **77**, 5508 (1982); (g) M. Roy and T. B. McMahon, *Org. Mass Spectrom.* **17**, 392 (1982); (h) S. Nourbakhsh, K. Norwood, G.-Z. He, and C. Y. Ng, *J. Am. Chem. Soc.* **113**, 6311 (1991); (i) B. Ruscic and J. Berkowitz, *J. Chem. Phys.* **97**, 1818 (1992); (l) L. A. Curtiss, R. H. Nobes, J. A. Pople, and L. Radom, *ibid.* **97**, 6766 (1992); (m) R. H. Nobes, and L. Radom, *Chem. Phys. Lett.* **189**, 554 (1992); (n) J. R. Flores, C. Barrientos, and A. Largo, *J. Phys. Chem.* **98**, 1090 (1994).
- <sup>2</sup>(a) D. R. Yarkony, in *Atomic, Molecular, and Optical Physics Handbook*, edited by W. F. Drake and M. Gordon (AIP, Woodbury, New York, 1996), p. 357, and references therein; (b) J. C. Lorquet, in *The Structure and Energetics of Organic Ions*, edited by T. Baer, C. Y. Ng, and I. Powis (Wiley, New York, 1996); (c) H. Nakamura, *Annu. Rev. Phys. Chem.* **48**, 299 (1997); (d) E. E. Nikitin, in *Ref. 2a*, p. 561, and references therein.
- <sup>3</sup>M. Aschi, J. N. Harvey, C. A. Schalley, D. Schröder, and H. Schwarz, *J. Chem. Soc. Chem. Commun.* **1998**, 532.
- <sup>4</sup>The experimental evidence pointed out the larger efficiency of reaction (3a).

- <sup>5</sup>(a) A. D. Becke, *J. Chem. Phys.* **98**, 5648 (1993); (b) P. J. Stephens, F. J. Devlin, C. F. Chabalowski, and M. J. Frisch, *J. Phys. Chem.* **98**, 11623 (1994); (c) C. Lee, W. Yang, and R. G. Parr, *Phys. Rev. B* **37**, 785 (1988).
- <sup>6</sup>M. J. Frish, J. A. Pople, and J. S. Binkley, *J. Chem. Phys.* **80**, 3265 (1984).
- <sup>7</sup>(a) R. J. Bartlett and G. D. Purvis, *Int. J. Quantum Chem.* **14**, 516 (1978); (b) K. Raghavachari, G. W. Trucks, J. A. Pople, and M. Head-Gordon, *Chem. Phys. Lett.* **157**, 479 (1989).
- <sup>8</sup>(a) T. H. Dunning, *J. Chem. Phys.* **90**, 1007 (1989); (b) R. A. Kendall, T. H. Dunning, and R. J. Harrison, *ibid.* **96**, 6796 (1992); (c) D. E. Woon and T. H. Dunning, *ibid.* **98**, 1358 (1993).
- <sup>9</sup>D. McQuarrie, *Statistical Mechanics* (Harper and Row, New York, 1976).
- <sup>10</sup>GAUSSIAN 94, M. J. Frisch, G. W. Trucks, H. B. Schlegel, P. M. W. Gill, B. G. Johnson, M. A. Robb, J. R. Cheeseman, T. A. Keith, G. A. Petersson, J. A. Montgomery, K. Raghavachari, M. A. Al-Laham, V. G. Zakrzewski, J. V. Ortiz, J. B. Foresman, J. Cioslowski, B. B. Stefanov, A. Nanayakkara, M. Challacombe, C. Y. Peng, P. Y. Ayala, W. Chen, M. W. Wong, J. L. Andres, E. S. Replogle, R. Gomperts, R. L. Martin, D. J. Fox, J. S. Binkley, D. J. Defrees, J. Baker, J. P. Stewart, M. Head-Gordon, C. Gonzalez, J. A. Pople, Gaussian, Inc., Pittsburgh, PA, 1995.
- <sup>11</sup>(a) D. R. Yarkony, in *Modern Electronic Structure Theory*, edited by D. R. Yarkony (World Scientific, Singapore, 1995), p. 642; (b) N. Koga and K. Morokuma, *Chem. Phys. Lett.* **119**, 371 (1985); (c) M. Bearpark, M. A. Robb, and H. B. Schlegel, *ibid.* **223**, 269 (1994).
- <sup>12</sup>J. N. Harvey, M. Aschi, H. Schwarz, and W. Koch, *Theor. Chem. Acc.* **99**, 95 (1998).
- <sup>13</sup>M. W. Schmidt, K. K. Baldrige, J. A. Boatz, S. T. Elbert, M. S. Gordon, J. H. Hensen, S. Koseki, N. Matsunaga, K. A. Nguyen, S. J. Su, T. L. Windus, M. Dupuis, and J. A. Montgomery, *J. Comput. Chem.* **14**, 1910 (1993).
- <sup>14</sup>S. Koseki, M. W. Schmidt, and M. S. Gordon, *J. Phys. Chem.* **96**, 10768 (1992).
- <sup>15</sup>(a) P. J. Robinson and K. A. Holbrook, *Unimolecular Reactions* (Wiley, New York, 1971); (b) T. Baer and W. Hase, *Unimolecular Reaction Dynamics* (Oxford University Press, New York, 1996).
- <sup>16</sup>W. H. Miller, *J. Am. Chem. Soc.* **101**, 6810 (1979).
- <sup>17</sup>(a) J. C. Light, *J. Chem. Phys.* **40**, 3221 (1964); (b) C. Klots, *Z. Naturforsch. A* **27**, 553 (1972); (c) W. J. Chesnavich and M. T. Bowers, *J. Am. Chem. Soc.* **99**, 1705 (1977); (d) D. M. Wardlaw and R. Marcus, *Adv. Chem. Phys.* **70**, 231 (1988); (e) S. J. Klippenstein, J. D. Faulk, and R. C. Dunbar, *J. Chem. Phys.* **98**, 243 (1993).
- <sup>18</sup>W. Forst, *Theory of Unimolecular Reactions* (Academic, New York, 1973), Sec. 6.8.
- <sup>19</sup>J. C. Lorquet and B. Leyh-Nihant, *J. Phys. Chem.* **92**, 4778 (1988).
- <sup>20</sup>J. N. Harvey and M. Aschi, *Phys. Chem. Chem. Phys.* (submitted).
- <sup>21</sup>J. B. Delos and W. R. Thorson, *Phys. Rev. A* **6**, 728 (1972).
- <sup>22</sup>M. Abramowitz and I. A. Stegun, *Handbook of Mathematical Functions* (Dover, New York, 1975).
- <sup>23</sup>Briefly, following the initial check of the singlet and triplet gradients, independent optimizations leading to the expected minima or exit channels have been carried out on the two surfaces. See, for example: D. Schröder, C. Heinemann, H. Schwarz, J. N. Harvey, S. Dua, S. J. Blanksby, and J. Bowie, *Chem.-Eur. J.* **4**, 2550 (1998).
- <sup>24</sup>All the calculated rate constants are available as additional material upon request.
- <sup>25</sup>(a) J. L. Holmes, *Org. Mass Spectrom.* **20**, 1669 (1985); (b) B. A. Rumpf and P. J. Derrick, *Int. J. Mass Spectrom. Ion Processes* **82**, 239 (1988); (c) F. Grandinetti, *Org. Mass Spectrom.* **28**, 1504 (1993).